Improved Efficiency of Microcrystalline Silicon Thin Film Solar Cells with Wide Band-Gap CdS Buffer Layer

M. Jabeen[1], S. Haxha, Senior Member, IEEE and M.D.B Charlton

[1]Department of Computer Science and Technologies, University of Bedfordshire, University Square, Luton, Bedfordshire, LU1 3JU, United Kingdom.
[2]Electronics and Computer Science, University of Southampton University Road Southampton SO17 1BJ.
**shyqyri.haxha@beds.ac.uk*

Abstract: In this paper, we have reported a new structure based upon an optical simulation of maximum light trapping and management in microcrystalline silicon thin film solar cells by using multi texture schemes and introducing an n-type cadmium sulphide (CdS) buffer layer with the goal of extreme light coupling and absorption in silicon absorber layer. Photon absorption was improved by optimising the front and back texturing of transparent conductive oxide (TCO) layers and variation in buffer layer thickness. We have demonstrated that light trapping can be improved with proposed geometry of *1µm* thick crystalline silicon absorber layer below a thin layer of wide band gap material. We have improved the short circuit current densities by *1.35mA/cm²* resulting in a total short circuit current of *25 mA/cm²* and conversion efficiency of *9%* with the addition of CdS buffer layer and multi textures, under global AM*1.5* conditions. In this study, we have used 2 Dimensional Full Vectorial Finite Element (2DFVFEM) to design and optimize the proposed light propagation in solar cell structure configuration. Our simulation results show that interface morphology of CdS layer thickness and textures with different aspect and ratios have the most prominent influence on solar cell performance in terms of both short circuit current and quantum efficiency.

Index Terms: Cadmium sulphide, Solar Cells, µc-Si thin film solar cells, Improved Efficiency.

1. Introduction

Thin film technology is one of the most promising development in photovoltaic research. High conversion efficiency can be achieved through various significant light trapping strategies including nanoparticles at substrate surfaces, Nanorods/Nano tubes, and introducing photonic crystals in absorber or transparent layers [1-6]. Most common and effective approach is surface texturing at front or back contact to enhance incoupling and scatterings of light [3, 4]. Silicon thin films are bad absorber and do not absorb sufficient light in visible range and for longer wavelengths in *600-800nm* range. Improving absorption efficiency of thin film silicon solar cells is thus a crucial part for photovoltaics, thus different practical methods and Nano techniques have been developed for photon management in random or periodic textured silicon solar cells and nanocrystals in superstrate or substrate configurations [5, 7, 8]. The amorphous silicon version has relatively poor efficiency that is due to low photocurrent generation and tendency to be unstable except some interface morphologies and surface configurations to improve light absorption [9-11]. PV cells made of CdTe/CIGS semiconductor material often combinations of complex compounds have been reported as good light absorber in terms of cost and efficiency effectiveness based on their bandgap well matched ability to the normal sunlight [12-14]. PV Such complex combinations of semiconductor compounds have been extensively used by many research groups and competitive PV teams to optimize the band gap and to increase the light absorption. Different methods have been established to derive optimal surface textures in silicon thin films solar cells to provide a good settlement between light incoupling at short wavelengths and maximum light trapping at long wavelengths [4, 8]. So far, the best performing nanostructure thin film materials including polycrystalline silicon are considered reasonable in terms of fabrication cost effectiveness and overall efficiency (which strongly relies on randomly textured substrates) [15]. Thus, the most effective way to increase the optical and electrical performance of solar cells, thin film solar cells was configured with periodic or random texturing of substrates along with thin transparent oxide [7,16-19]. For present era, it is important to achieve goals of coupling as much light as possible into thin film solar cells along with low cost fabrication and high-quality values, therefore current solar cells include back reflectors, anti-reflection

coatings, surface texturing and window or buffer layers as necessary elements for light management [20-25]. CdS is commonly used as buffer layer material in thin film solar cells along with Copper-Indium-Gallium-Selenide (CIGS) and Cadmium-telluride (CdTe) absorber materials due to its wide band gap properties [12,13,26]. Thin films of CdS with high n type polarity are the most appropriate material as carrier transport layers and has significant effect on conversion efficiency where thickness of these films leads to high short circuit current densities and enhanced absorption in absorber layers. To achieve high conversion efficiency of silicon solar cells, different bandgap material layers are stacked together to form sufficient light trapping solar cells, therefore those layers respond to different wavelength ranges and lead to maximum absorption for whole sun spectrum. [27-32].

Regarding multi textured crystalline silicon based solar cells there have already been some promising simulated and experimental work published using optimizations of front and back contact texturing and morphologies of plasmonic losses in back reflectors [33-35]. This manuscript basically presents the simulation study of improved light trapping in textured microcrystalline silicon solar cells with the combination of thin transparent CdS buffer layer, thus achieved results are more plausible as discussed in [36].

In this simulation based work we explored the possibilities of maximum light trapping effects achieved by adding another transparent CdS thin buffer layer above crystalline silicon absorber layer and texturing of front and back Transparent Conductive Oxide (TCO) layers made of aluminium doped zinc oxide (ZnO: Al). The proposed solar structure shows major improvements in terms of key performance indicators such as quantum efficiency (QE) and short circuit current density (Jsc).

2. Purposed Structure

The proposed cross sections of microcrystalline silicon solar cells are illustrated shown in Fig. 1. Since 2D space dimension was used with a direct solver method and reasonable degrees of freedom was taken into considerations. The simulated structure based on μc-Si absorber material has following layer assembly: Ag (*100nm*) / BTCO(*200nm*) / μc-Si (*1μm*) / CdS(*180nm*) / FTCO(*340nm*) / Thin protective glass layer(*50nm*) / Air medium($\lambda/2$). The front and back TCO are Aluminum doped zinc oxide semiconductor (ZnO: Al). The μc-Si pin diode consists of *20nm* p-layer, *20nm* n-layer and *1μm* i-layer [8, 15, 36, 37]. The optical properties of materials used in solar cell structure were defined by complex function of wavelength dependent refractive indexes (ε) and values were taken from well-known literature [38-43]. Details on the values of refractive index and utilized optical parameters are as follows in Table 1 [44].

Table 1: The utilized values of parameters and their structural and optical properties.

Parameters and layers optical properties	**Value**	**Parameters and layers optical properties**	**Value**	**Parameters and layers optical properties**	**Value**
T_0 (Temperature)- Ref [39,40]	*300[K]*	Effective density of state valence band, CdS -Ref [39,40]	*1.8E19[1/cm^3]*	Electron diffusivity in CdS(Dn_CdS)-Ref [39]	*9 [cm^2/s]*
N_i (intrinsic carrier concentration)- Ref [39,40]	*1.5E10[1/cm^3]*	Effective density of state conduction band, CdS-Ref [39,40]	*2.4E18[1/cm^3]*	Hole diffusivity in CdS(Dp_CdS)-Ref [39]	*1.4 [cm^2/s]*
N-doping	*1E17[1/cm^3]*	Effective density of state valence band, c-Si -Ref [39,40]	*1.8E19[1/cm^3]*	Angle of incident light	*0[deg]*
P-doping	*1E17[1/cm^3]*	Effective density of state conduction band, c-Si-Ref	*3.2e19[1/cm^3]*	Electron affinity (CdS)-Ref [39]	*4.3[V]*

		[39,40]			
Thickness (n-doped, c-Si) -Ref [36]	*20[nm]*	Diffusion length of electrons-Ref [40]	*0.2[um]*	E_g – CdS-Ref [39]	*2.42[V]*
Thickness (p-doped, c-Si)-Ref [36]	*20[nm]*	Diffusion length of holes -Ref [40]	*0.3[um]*	E_g - ZnO -Ref [39]	*3.37[V]*
Thickness (intrinsic, c-Si)-Ref [36]	*1[um]*	Electron affinity (c-Si)-Ref [39,40]	*4.05[V]*	Refractive index of c-Si-Ref [44]	*3.96*
Thickness (ZnO: Al, FTCO)-Ref [36]	*340[nm]*	Relative permittivity for CdS -Ref [39]	*8.9*	E_g - Si at 300[K])-Ref [39,40]	*1.75[V]*
Thickness (ZnO: Al, BTCO)-Ref [36]	*200[nm]*	Relative permittivity for silicon	*11.7*	CdS Refractive index -Ref [44]	*2.5*
Thickness(glass)	*50[nm]*	Electron mobility in CdS (mun_CdS)-Ref [39]	*340[cm^2/V*s]*	Refractive index of ZnO: Al-Ref [44]	*1.8284*
Thickness(Air)	*ʎ /2*	Hole mobility in CdS (mup_CdS) -Ref [39]	*50 [cm^2/V*s]*	Glass Refractive Index-Ref [44]	*1.5*
Thickness(Ag)-Ref [36]	*100[nm]*	Air Refractive Index-Ref [44]	*1.000293*	Ag Refractive Index-Ref [44]	*0.051585*
Dielectric Constant of CdS $\varepsilon/\ \varepsilon_0$	*10*	n-type doping defect density of CdS	*1E17[1/cm^3]*	CdS distribution width	*0.1[eV]*

The 2DFVFEM simulations are carried out at wavelength range (*300nm-1100nm*). Based on variety of spatial dimensions there are 1D, 2D or 3D geometries for PV modelling. While for most thin film solar cell simulations the application of 1D and 2D models are significant because in 3D optical models the complexity of higher dimension simulation of textured or non-flat layers is significantly increased [4,10,45]. Thus, 2D finite element formulation normally solves quicker than other 3D solvers and also it offers wider degrees of freedom and several discretization modes for interfaces. Other Maxwell solvers like Finite Difference time domain FDTD method, boundary element method (BEM) and Fourier Model method (FMM) are also utilized for periodic structures to obtain high accuracy where FMM is used for homogeneous layers of simple structures. Although for complex geometries 2D/3D FEM is more precise, particularly for designing nanostructure photovoltaic cells where S-matrix calculations are quite time consumptive by 2DFVFEM. For our proposed solar cell structure simulations, we have exploited this PV simulator which provides high dimensional modelling of devices and can couple certain physics all together. The most appealing and advanced feature of 2DFEM formulation is the direct access discretization modes to solve partial differential equations via FEM or FVM with time dependent solver characteristics make it perfect solver to calculate performances of PV devices. In general, 2D model simulations continually solves quicker then 3D because for axi-symmetric geometries and boundary conditions 2D axi-simulations provides more easy and reasonable solutions then full 3D simulations.

In this research study, we have used FVFEM to investigate optical wave propagation within solar cell by using 2-D geometry where optical modes and the electric field distribution for normal incidence light

have been investigated. Electrostatics and transport of diluted species were used to analyze the applied and generated potential within solar cell and mobility and concentration of carriers respectively Frequency domain and stationary study steps were utilized to obtain carrier generation spectrum and I-V characteristics. Several equation models have been reported previously [39, 40] which are commonly used for the optical and electrical modelling and simulation of thin film solar cells.

Electrostatic potential and carrier density equations are fundamental equations and specifically linked together. The Poisson's equations, continuity equations and carrier transport equations are primarily derived from Maxwell's laws where partial differential Maxwell's equations are analytically solved for simple geometries [45].

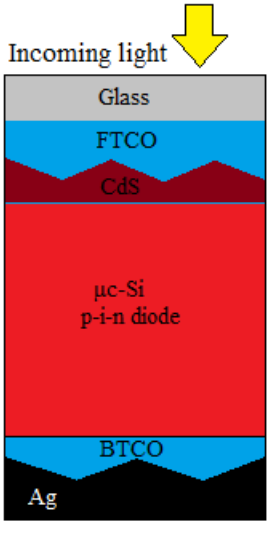

Fig. 1. Configuration of proposed solar cell structure with CdS buffer layer.

Glass substrates with randomly roughened Indium Tin Oxide (ITO) or Aluminum Zinc Oxide (AZO) (Front) Transparrent Contact Layers (TCL) with pyramidal features (as shown in fig 1) can be bought off the shelf from companies such as Pilkingtons. Roughening is by wet crystallographic chemical etch process. Our designs would require a simple patterned etch process such as greyscale masked contact lithography, followed by isotropic wet etch process. Microcrystalline solar cell layers would then be grown by Chemical Vapour Deposition direct onto the patterned TCO layer. The back TCL would then be deposited by reactive sputtering or e-gun evaporation process, followed by e-gun evaporation of the silver rear reflector layer.

Where needed, conformal layers of CDs material could be deposited by Chemical Bath Deposition (CBD) direct onto the pre patterned TCO layer.

Mobility model, Shockley read hall recombination model, Lifetimes and diffusion of carriers were solved consistently where we calculated short circuit current density by using Eq. (1). The current-voltage (I-V) curve of solar cell under illumination are ideal features which was derived from dark current curve shifted by an amount of generated photon current shift factor $Aq\,(G\text{-}R_{srh})$ given below [40]:

$$I_{Light}(V) = I_{Dark}(V) - Aq(G(\tau_{n} + \tau_{p})) \tag{1}$$

where A is the active area of solar cell, q is elementary charge, G is generation term, R_{srh} is recombination rate, τ_n and τ_p are carrier life time of electrons and holes, respectively. The electric field amplitude of incident wave was taken *1*V/m. Time average power loss $Q\,(x, y, z)$ in a node within absorber domain was calculated via electric field distribution by using following equation [38].

$$Q(x, y, z) = \frac{1}{2} c\varepsilon_0 \eta\alpha \left|E(x, y, z)\right|^2 \tag{2}$$

where c is the speed of light, ε_0 is free space permittivity, α is the absorption coefficient ($\alpha = 4\pi\kappa/\lambda$) with κ being the imaginary part of complex refractive index, η is the real part of complex refractive index, λ is the wavelength and $E\,(x, y, z)$ is the electric field strength at corresponding excitation wavelength. Quantum Efficiency (QE) is the ratio of generated and collected charge carriers by total incident photons. In our simulations, we assumed that internal quantum efficiency is *100%* and all charge carriers that

generate in p-i-n stack were collected. Furthermore, in our simulations electrical losses were not considered and detailed calculations of quantum efficiency and short circuit current are given in literature [34]. Hence, simulated external quantum efficiency was calculated as a ratio of total power absorbed in absorbing layer by total optical incident power P_{opt} [34, 38]:

$$QE = \frac{1}{P_{opt}} \iiint Q(x, y, z)dxdydz \tag{3}$$

In literature, there are several complex models that describe the thin film layers and textures growth for silicon based solar cells considering combination of isotropic and conformal growth. Triangular (pyramid shaped) textures of solar cell has been explored for front and back transparent layers and these pyramid shaped textures were placed normal to substrate boundaries as depicted in Fig. 1. Textures height was kept constant at *300nm* and textures period used *1.1um* and *1.2um* consecutively. Buffer layer thickness was varied frequently to optimize the absorption enhancement and short circuit current effects.

Excitation in the form of vertically plane incident wave was generated at top boundary of air domain by using Lumped Port (RF module) boundary condition. The entire domain was finely meshed for electromagnetic wave propagation. Since the port boundary condition has specific properties for maximum absorption of incident waves reducing the possibilities of multiple reflections. Model width was set according to the period of multiple textures. The incident irradiation power was kept constant for all the simulations. Periodic and floquent boundary conditions were used on left and right boundaries of solar cell to optimize the refraction effects of incident light through each material of solar cell. The simulated absorption is scaled to AM *(1.5*) sun's spectral irradiance which is *1000W/m^2 (100mW/cm^2),* details of these standard values are given in literature [46].

3. Results and Discussions

Prior to the proposed textures silicon solar cell with improved structure, *μ*c-Si solar cell with single front and back texture and multi front textures in TCO layers. We have benchmarked our model with experimental obtained results in Ref. [36], the simulations were performed by using structure shown in Figs. 5(a) and 5(b) in Ref [36]. The I-V characteristics of single and multi-textures solar cells are presented in Fig. 3 where the electrical simulation results are described in Table 2. Furthermore *μ*c-Si solar cell structure was improved by using n-type CdS buffer layer with different thicknesses. Most promising results were achieved with CdS layer thickness *180nm* and specific texture period of *1.1μm* and *1.2μm* in Front and back TCO layers and texture thickness was kept constant at *300nm*. The quantum efficiency was simulated under short circuit current conditions by using power loss profile shown in Figs. 2 and 6(a). The Improved structure exhibited low absorption for short wavelengths (*300-450nm*) and several high absorption peaks were observed for long wavelengths *(>600nm)*.

3.1. Analysis of Simulated results with single texture and multi-textures without buffer layer

We have simulated and analyzed a plane solar cell structure and our simulations show low QE (*5%*), Therefore due to low QE we have not included the schematics and the results in this paper. Surface roughness and texture creation is a vital factor to increase light trapping and absorption specifically in silicon thin film solar cells. Therefore, in most cases surface textures are designed in transparent substrates or conductive oxide films located at top and bottom of semiconductor absorber layer. According to latest studies the specific pyramid or cone shaped textures in TCO films can increase surface roughness and light trapping as well as direct extra light to the absorber layer by making it further transparent to the device [5,47,48]. The period and thickness of textures depends upon thickness of TCO layer and directly affect the transmissions and reflections of photons.

The thin film *μ*c-Si solar cell can be schematically depicted in Fig. 1. As less thickness of TCO layer can produce less surface roughness, for this model the FTCO (ZnO: Al) layer thickness is *340[nm*]. For opto_electric conversion, a p-i-n stack made of μc-Si has been considered where thickness of intrinsic layer used to be *1μm* and p layer and the n layer *20nm* thick [36].

To analyse the effects of buffer layer in textured *μ*c-Si solar cell structure, we have investigated two sets of solar cells, by using the same thickness of *μ*c-Si active layer for all simulations. Initially we simulated two structures one with single front and back texture in TCO layer and second with multi front textures without buffer layer as baseline and finally demonstrated an evocative comparison of the *μ*c-Si pin solar cell that was simulated by different thicknesses of additional CdS buffer layer and textures in TCO layers. The *μ*c-Si pin solar cells were characterized by measuring their current density (J-V) characteristics and quantum efficiency (QE) under AM1.*5* illumination by using data from standard solar

spectrum. The open circuit voltage and short circuit current for single textured and multi textured simulated benchmark structure was obtained *0.5mV*, *20mA/cm²* and *0.5mV*,*22mA/cm²* respectively and can be perceived in Fig. 3. The contribution of generated current at different wavelengths by means of solar cell efficiency and Fill Factor (FF) for simulated pin structure are listed in Table 2 where the maximum QE occurred at *560nm* wavelength. To investigate the effect of single texture and multi texture interfaces of TCO, solar cells with texture variation were simulated. In the first step of simulation *μ*c-Si solar cells with single front and back texture were analyzed. Second step of simulation was based on simulation of *μ*c-Si solar cell with multiple textures in TCO layer whereas front boundary of TCO for light incoming to solar cell was kept flat. The calculated short circuit current and quantum efficiency for first and second step simulations are depicted in Table 2.

Table 2. Comparison between the characteristics of the reference cell and simulated cell.

Parameters	**Reference multi textured Cell [36]**	**Simulated single textured Cell**	**Simulated multi textured Cell**
V_{OC} (mV)	*0.515*	*0.5*	*0.5*
J_{SC} (mA/cm2)	*23.65*	*20*	*22*
Fill factor (*%*)	*69*	*71*	*72*
Conversion Efficiency (*%*)	*8.35*	*7.14*	*7.92*

In *μ*c-Si solar cell with single front and back texture, the generated current was found to be minimum for blue spectral region (*300-400nm*) and increased significantly in visible region range(*400-600nm*) and gradually decreased in remaining spectrum region (*600-1000*) by means of solar cell efficiency as shown in Fig. 2. To obtain quantum efficiency curve the simulations were run at every single wavelength from 300nm to *1100nm* with the step difference of *10nm*. It was observed that single and multi-front textures have significant impact on efficiency enhancement within the range of *450nm -650nm*. The period of single front and back texture was used *3μm* while the height of single texture was kept *0.2μm*. Significant increase in efficiency in wavelength ranges *450-650nm* is indicative of relevant increase in light path, therefore more light couples within the absorber layer due to specific shape and size of single texture. According to recent reports from literature, the most efficient way to develop an optimal thin silicon absorber layer is to use invert pyramid shape texture equal to the value of *λ/2n or λ/4n* (*λ*: incident beam wavelength, *n*: refractive index) in TCO film to channel the maximum light into the active layer [49]. Referring this topology solutions, the TCO layer was shaped into wide cone wedge like texture to increase the amount of light enters the *μ*c-Si absorber layer as well as optimal texture thickness(*0.2μm,0.14μm*) that reduces excessive light reflections from surface of solar cell and enhances light transmissions through transparent oxide layers. Maximum light absorption for single texture solar cell simulation was achieved *7.14%* at wavelength *560nm* while there was no specific absorption for longer wavelengths at *700-900nm* recorded that is because of short wavelengths of light gets absorbed near to front surface of solar cell and due to single back texture longer wavelengths could not couple more efficiently and slightly scatter within absorber layer. Total short circuit current for single front and back texture can be perceived in Fig. 3.

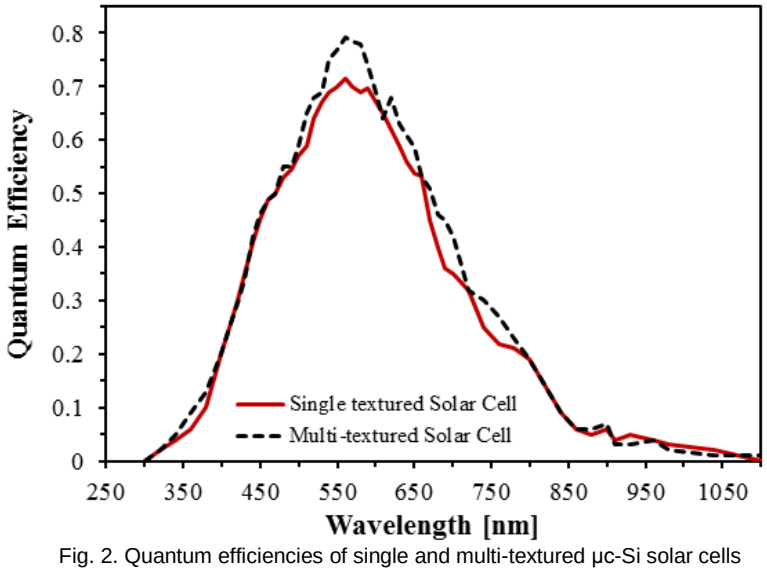

Fig. 2. Quantum efficiencies of single and multi-textured µc-Si solar cells

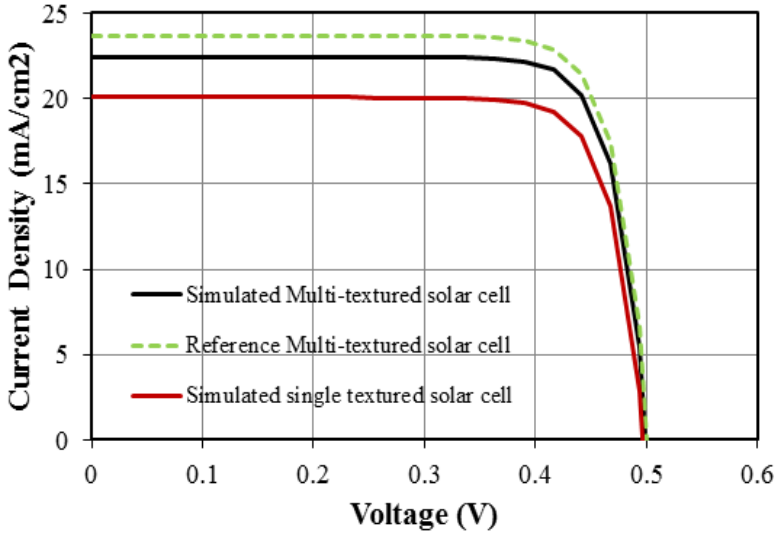

Fig. 3. Simulated benchmark optical and electrical properties of single and multi-textured *µc*-Si solar cells. Current/Voltage (I/V) curve and a comparison between simulated and measured data in Ref. [36] is shown in embedded *Table 2*.

In second step, the simulations were carried out by using multiple textures in front TCO layer and a single texture was used in back TCO to explore the optimal light trapping scheme. The period of front textures was kept at *1.1µm* and *1.2µm* consecutively, while the height of textures used was *200nm* as shown in Fig. 4.

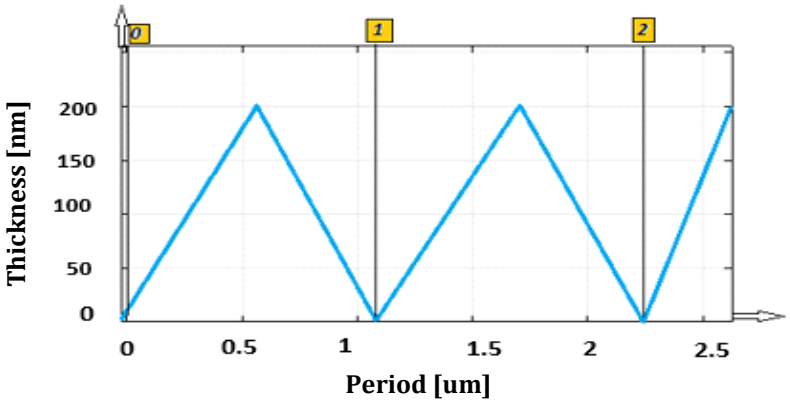

Period of 1st and 2nd texture	0-1	1-2
Horizontal distance	1.1um	1.2um
Vertical distance	200nm	200nm

Fig. 4. Texture cross section profile with respect to horizontal and vertical distance.

Although a single texture in back TCO was used with a period of *3μm* and height *0.16μm*. Hence these two sets of solar cells with single texture and front multitexture were used as benchmark simulated structures shown in Figs. 5(a) and 5(b). Significant improvement in short circuit current was measured and therefore QE was calculated for solar cell by using Eq. (2) and Eq. (3) with multitexture at front interface. For the solar cell structure, with different front textures, the short circuit current is increased by *2mA/cm²* and improved from *20mA/cm²*(for single front and back texture) up to *22mA/cm²*(for front multi textures and single back texture). This increase in short circuit current and solar efficiency with multi textures was because of light path increases due to multiple passes of scattered light within the solar cell which can be observed by perceiving interference fringes and diffraction of light in power absorbed and power loss profiles of analyzed structures shown in Fig. 5. In addition to light scattering, and deflection more competently at textured interfaces, photonic resonances may contribute to light trapping in the absorber layer. Although partial loss in coherence of scattered light at highly textured interfaces as vital aspect was observed in terms of reduced interference fringes and reflection losses. Therefore, some coherency approaches including phase elimination and phase matching techniques can be carried out to slightly maintain coherency of scattered light [22, 50]. Consequently, when switching from single textured to multi textured TCO interface the increase in current density (ΔJ_{SC}) was *2mA/cm²* (Fig. 3) and an increase in conversion efficiency (*ΔE*) *0.78%* from *7.14%* to *7.92%* (Fig. 2) was recorded for the same thickness of TCO and absorber layer as summaries in Table 2.

3.2 Analysis of Simulated results with multi-textures and buffer layer

Next stage of simulation was to analyse the effect of adding buffer layer at top of absorber layer that would enhance the solar cell efficiency by coupling maximum light and preventing extra absorption and recombination at other interfaces of the solar cell. In our model, a thin film of n-type cadmium sulphide (CdS) buffer layer was used in xy plane to investigate the effect of thin film onto short circuit current and quantum efficiency of *μ*c-Si solar cell. Several research groups have found that optimisation of solar cell layers' performance can be significantly increased by utilising the materials with less than ideal properties to achieve best performance of solar cell [49]. There are several imperative factors including Enhanced recombination of photo generated carriers at defects, and low minority carrier life time can reduce the overall performance of solar cell [51]. Thus, embedding a buffer layer at specific position of solar cell interface is another way to enhance solar cell performance in terms of short circuit current and conversion efficiency [26, 27, 51, 52]. Generally graded or gradual buffer layer seems to increase open circuit voltage (Voc) of solar cells with diverse interaction processes such as interface or interface diffusive or mobility properties. However, there are several ways available to insert buffer layers to enhance overall efficiency of solar cells including, Buffer layer with band alignment to absorber layer, Buffer layers inside p-i-n interfaces like graded layer to increase Voc, and Buffer layers without band alignment for minority carriers but for majorities to block back diffusion of electrons in p-i-n silicon layer and to allow them to flow to the

contact so that they will be collected by collector safely [51, 52].

In our model, we used buffer layer that prevents photoexcited carriers' recombination at wrong places like at TCO or contacts instead of absorber layer [51]. We investigated the general effect of adding this buffer layer at top of *μ*c-Si absorber layer to investigate what effect it could possibly offer to short circuit current and to overall conversion efficiency of *μ*c-Si solar cell. A very thin layer of Cadmium sulphide was added at top of p-i-n *μ*c-Si absorber layer and the influence of this layer was investigated by using different thicknesses of buffer layers at, *180nm*, *130nm*, and *70nm*. A good agreement was achieved for CdS layer thickness at *180nm* and same structure dimensions for multitexture solar cell was used as discussed in step 2 simulations. The texture thickness used to be *300nm* and texture period was kept at *1.1um* and *1.2um* consecutively for both FTCO layer and BTCO layers and similar thickness of p-i-n μc-Si absorber layer stack was used at *20nm,1um,20nm* respectively as shown in Fig. 5(c). The interference fringes in terms of spectral position and power profiles found in good promise and showed a correct demonstration of optical path throughout solar cell as demonstrated in Fig. 5(d-f). However, a minor change in absorption amplitude was observed for long wavelengths above *600nm* which might be due to material dispersive losses or out coupling of light from peripheral areas of solar cells [53].

By using global performance parameters like short circuit current and quantum efficiency, a comparison of thickness variation may be more effective to observe operation of additional layer under illumination conditions. Therefore, we calculated quantum efficiency over photocurrent generation region by integrating the power losses over *μ*c-Si absorber region dividing this power loss in absorber layer spectra by total incident optical power as described in Eq. (3). The power loss profiles showed that longer wavelength light at *680nm* reaches the Ag metal back, where some portion of light was absorbed, while most of the light was reflected Fig. 5(d-f). Moreover, for single texture cell there is low scattering throughout absorber layer (Fig. 5(d)), for multitexture solar cell power absorption and diffraction was slightly more observable (Fig. 5(e)), while for multitexture solar cell with the addition of CdS buffer layer more effective power absorption and scattering was obvious as shown in Fig. 5(f).

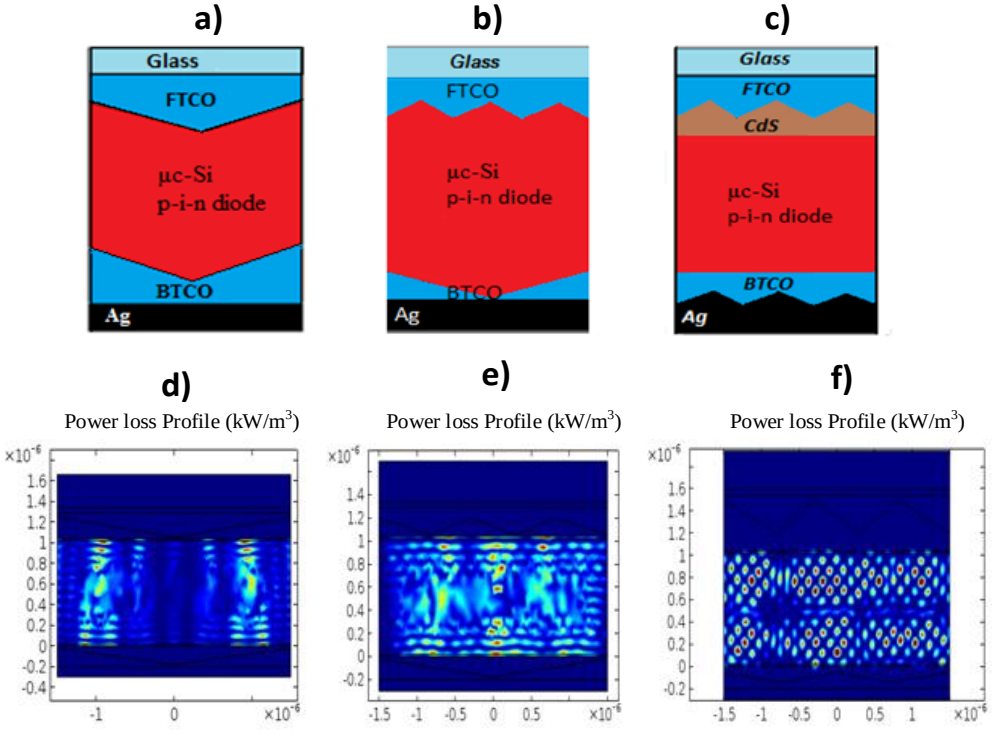

Fig. 5. Cross sections and power loss profiles of solar cells. (a) single textured solar cell (b) Multitexture solar cell (c) proposed multitexture solar cell with CdS buffer layer (d-f) Respective power loss profiles at *680nm* wavelength.

In following optical simulations of solar cell, material and optical properties used for cadmium sulphide CdS layer are specified in literature [12, 27]. Where the optical absorption coefficient for CDS thin films was calculated by using equations from literature [54]. Absorption coefficient of CdS is related to film

thickness and absorbance which indicates that as we increase the film thickness the optical energy gap (E_g) of CdS decreases [54]. Thus, the simulation results were carried out by defining variables including wavelength dependent Absorption coefficients (α) of considering materials. ZnO: Al was used as Transparent conductive oxide to reduce series resistance which might arise due to small thickness of Cadmium sulphide layer. Invariably CdS is n-type material and has wide band gap (E_g ~ *2.4 eV* at *300K*) therefore it can be turned into more transparent layer for long wavelengths and can be used as window layer or buffer layer. Optical absorption of CdS depends upon wavelength but performance of solar cells with buffer layer also depends slightly onto specific buffer layer thickness assortment [29,51,52,54]. Thus, to investigate the effect of CdS layer initially we simulate the μc-Si solar cell by using three different thickness of buffer layer *70nm,130nm* and *180nm* and designing back textures with same period as for front textures to investigate whether thickness could offer best performance effects. The I-V curve in Fig. 6(b) shows that maximum current density was obtained for thickness at *180nm* and the extracted parameters are shown in Table 3.

Table 3. Electrical Parameters of Solar Cell with Different Buffer Layer Configurations.

Different Buffer Layer Configuration	**Open Circuit Voltage(V_{oc})**	**Short Circuit Current (*mA/cm²*))**	**Fill Factor**	**Conversion Efficiency (%)**
CdS layer thickness *180[nm]*	*0.5*	*25*	*72*	*9.0*
CdS layer thickness *130[nm]*	*0.49*	*18.5*	*78*	*7.14*
CdS layer thickness *70[nm]*	*0.5*	*22.5*	*74*	*8.34*

Further integrating photon generated current over absorber layer nodes was calculated in terms of short circuit current density (J_{sc}). In Fig. 6(a) we showed the resulting Quantum efficiency spectra of solar cells, which was calculated with different thicknesses of CdS layer. By comparing these resulting graphs with previous simulated work in Fig. 2, a general statement can be observed. We noticed that absorption was still quite low, below *400nm* wavelength and that in *400-500nm* wavelength rang a significant improvement was found for all three-thicknesses used. However, this absorption spectra could be characterized by some oscillation effects above wavelength range *500nm* and maximum efficiency was observed at *560nm* wavelength for CdS thickness *180nm*. In contrast, for long wavelength range above *600nm*, a significant improvement in absorption was noticeable by means of small absorption fluctuating peaks because CdS material becomes more transparent down to long wavelengths. For small thickness of CdS up to *70nm*, good absorption spectra were indicative of a relevant increase in light path due to constructive interference of optical waves, therefore minimize the optical reflections losses and enhanced absorption in absorber layer, resulting in short circuit current of *22.5mA/cm²* and conversion efficiency *8.34%.* While that for thickness *130nm*, low absorption might reveal the fact that optical reflections losses and absorption at other interfaces increased and due to low optical path length absorption in absorber layer decreased, resulting short circuit current of *18.5mA/cm2* and conversion efficiency of *7.24%.* High QE and absorption for longer wavelengths with thickness up to *180* and *>180* was observed while for small thickness up to *70nm* high short circuit and current and maximum QE revealed the fact that low optical reflection losses occurred which cause improvement in scattered light path [32,38]. A gain in short circuit current of *1.35mA/cm2* was achieved for multitexture μc-Si solar cell with *180nm* thick CdS buffer layer yielding fill factor *72%* and conversion efficiency of *9.0%* compared to multitexture μc-Si solar cell mentioned in literature [36].

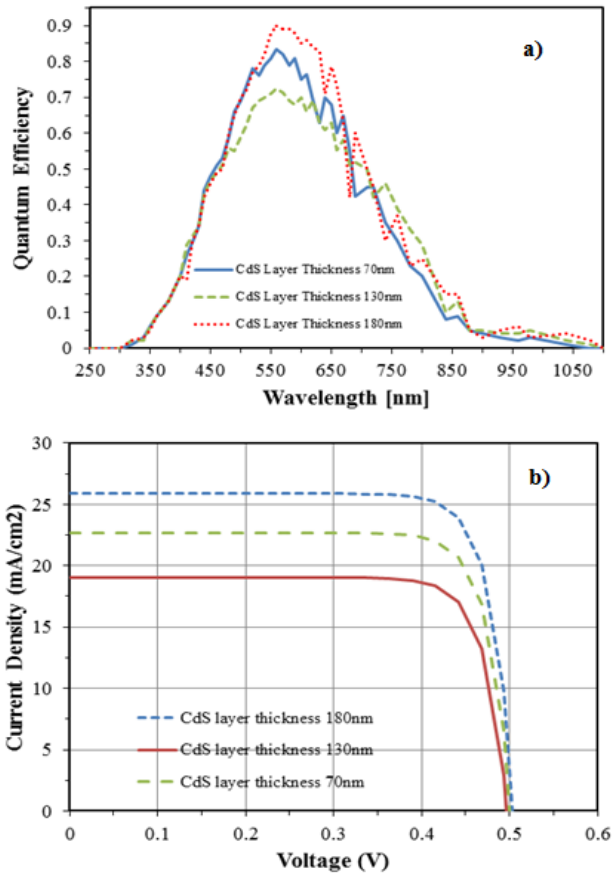

Fig. 6. A comparison between spectra obtained for Different thickness of CdS buffer layer for Overall Efficiency of μc-Si absorber layer. (a) Quantum Efficiency (b) Current-Voltage (I-V) characteristics.

Hence, we assumed that all the absorbed power produce good carrier excitation and generated carriers were collected perfectly. From Figs. 6(a) and 6(b) we concluded that quantum Efficiency and short circuit current measurement was effected not only by electrical properties of p-i-n junction but also due to the optical characteristics of supporting materials.

Overall, the short circuit current and quantum efficiency remains in good agreement with maximum recording obtained Short circuit current value of *25mA/cm²* and the conversion efficiency of *9.0%* has been gained with buffer layer of thickness *180nm* (Fig. 6).

From our observed absorption spectra, it is easily understandable that correct estimation of feature sizes of additional buffer layer during solar cell design strongly effects the spectral absorption peaks and hence increase the overall efficiency of solar cell [32,38,54], which briefly summarizes in Table 4.

Table 4. Guideline for optimisation of the Buffer layer effect on silicon thin film solar cell.

Buffer Layer thickness (Texture period *1.1um,1.2um*)	**Effect**	**Short Circuit Current density**	**Wave propagation and absorption**	**Overall Efficiency**
180-200[nm], >200nm	Longer wavelengths propagate and maximum coupling of light in absorber layer	High	Good absorption	Excellent

100-150[nm]	Low coupling of light due to interference losses and increased reflections.	Low	Low absorption	Average
< 100[nm]	Long wavelengths propagate efficiently and scatter throughout absorber layer.	High	Good absorption	Good

The effects of analyzed type of buffer layer could not be calculated analytically. This buffer layer has an impact on majority band configuration and barriers for minority carriers. Thus, this CdS buffer layer provides an optimum strategy to prevent motion of photoexcited minority carriers into wrong direction and therefore prevent their recombination at other interfaces resulting in an improved minority carrier lifetime. Based on these results it can be concluded that light management introduced by addition of buffer layer at top of absorber layer of solar cell stack has led to considerable decrease in outer reflections resulting an overall light absorption in absorber layer. Consequently, this buffer layer in *µ*c-Si structure also serves as an optical window with higher bandgap and low refractive index for increased coupling of light into the absorber layer resulting in an increased short circuit current and conversion efficiency.

4. Conclusions

In this paper, we have demonstrated a new solar cell structure which specified that light trapping and absorption in thin film solar cells based on 1µm thick µc*-Si absorber layer can be significantly improved with the addition of CdS buffer layer with explicit feature size and front and back textures in TCO layers. In our simulation based work we discussed three conditions to optimize light scattering and absorption in p-i-n stack with and without buffer layer. The impacts of performance of solar cell with variable texture period and buffer layer thickness are investigated. Initially simulations were performed using single texture and multi texture structures without buffer layer. Finally, three different thicknesses of CdS layer along with multi textures were investigated to observe their optical properties. By using FVFEM we have shown that buffer layer with 180nm thickness couples the light more efficiently in absorber layer and scattering of long wavelength light increases due to front and back textures.* In our proposed geometry (case (c)), the absorption of light in µc-Si absorber layer increased due to maximum scattering of light since top and bottom TCO textures together with CdS buffer layer attribute to increase short circuit current and interface recombination reduction. Significant results for improved solar cell performance is obtained when the buffer layer was used to be *180nm* thick. Whereas case (a) and (b) studies without buffer layer provide general optimization of linear structures exhibiting low conversion efficiencies up to *7.92%. We have observed that benefits of buffer layer arise since they couple the maximum light into absorber layer due to the fact that this layer has wide bandgap consequently it aligns band for majorities and minimize recombination at contact interfaces. Moreover, when this buffer layer is used near top of cell, optical enhancement is observed with the reduction of optical reflections. We have achieved higher short circuit current and quantum efficiency by using multitexture solar cell with texture period 1.1µm and 1.2µm, texture thickness 300nm, and CdS buffer layer thickness 180nm. The multitexture solar cell with CdS buffer layer leads to an increase in short circuit current by 1.35mA/cm^2 and conversion efficiency by 0.65% resulting total current density 25mA/cm^2 and maximum conversion efficiency 9%.*

References

[1] J. Xavier, J. Probst, F. Back, P. Wyss, D. Eisenhauer, B. Lochel, E. Rudigier-Voigt, and C. Becker, “Quasicrystalline-structured light harvesting nanophotonic silicon films on nanoimprinted glass for ultra-thin photovoltaics,” *Opt. Mater. Express*, vol. 4, no. 11, pp. 2290–2299, 2014.

[2] Y. Zhang, B. Jia, Z. Ouyang, and M. Gu, “Influence of rear located silver nanoparticle induced light losses on the light trapping of silicon wafer-based solar cells,” *J. Appl. Phys.*, vol. 116, no. 12, 2014.

[3] W. Ho, S. Su, Y. Lee, H. Syu, and C. Lin, “Performance-Enhanced Textured Silicon Solar Cells Based on Plasmonic Light Scattering Using Silver and Indium Nanoparticles,” *Materials (Basel).*, vol. 8, no. 10, pp. 6668–6676, 2015.

[4] K. Jäger, D. N. P. Linssen, O. Isabella, and M. Zeman, “Ambiguities in optical simulations of nanotextured thin-film solar cells using the finite-element method,” *Opt. Express*, vol. 23, no. 19, p. A1060, 2015.

[5] Z. H. D. Uan, M. L. I. Eicheng, T. R. M. Wenya, P. F. U. Engfei, and Y. L. I. Ingfeng, “Effective light absorption and its enhancement factor for silicon nanowire-based solar cell,” *Appl. Opt.*, vol. 55, no. 1, pp. 117–121, 2016.

[6] Y. Li, M. Li, P. Fu, R. Li, D. Song, C. Shen, and Y. Zhao, “A comparison of light-harvesting performance of silicon nanocones and nanowires for radial-junction solar cells.,” *Sci. Rep.*, vol. 5, no. April, p. 11532, 2015.

[7] R. Dewan, S. Shrestha, V. Jovanov, J. Hüpkes, K. Bittkau, and D. Knipp, “Random versus periodic: Determining light trapping of randomly textured thin film solar cells by the superposition of periodic surface textures,” *Sol. Energy Mater. Sol. Cells*, vol. 143, no. July, pp. 183–189, 2015.

[8] M. Meier, U.W. Paetzold, M. Ghosh, W. Zhang, T. Merdzhanova, G. Jost, N. Sommer, S. Michard, and A. Gordijn, “Fabrication of light-scattering multiscale textures by nanoimprinting for the application to thin-film silicon solar cells,” *IEEE J. Photovoltaics*, vol. 4, no. 3, pp. 772–777, 2014.

[9] A. Tamang, A. Hongsingthong, P. Sichanugrist, V. Jovanov, M. Konagai, and D. Knipp, “Light-trapping and interface morphologies of amorphous silicon solar cells on multiscale surface textured substrates,” *IEEE J. Photovoltaics*, vol. 4, no. 1, pp. 16–21, 2014.

[10] A. Ghahremani and A. E. Fathy, “A three-dimensional multiphysics modeling of thin-film amorphous silicon solar cells,” *Energy Sci. Eng.*, vol. 3, no. 6, pp. 520–534, 2015.

[11] V. Jovanov, U. Palanchoke, P. Magnus, H. Stiebig, J. Hupkes, P. Sichanugrist, M. Konagai, S. Wiesendanger, C. Rockstuhl, and D. Knipp, “Light trapping in periodically textured amorphous silicon thin film solar cells using realistic interface morphologies.,” *Opt. Express*, vol. 21, no. S4, pp. A595-606, 2013.

[12] M. Sabaghi, A. Majdabadi, S. Marjani, and S. Khosroabadi, “Optimization of high-efficiency CdS/CdTe thin film solar cell using step doping grading and thickness of the absorption layer,” *Orient. J. Chem.*, vol. 31, no. 2, pp. 891–896, 2015.

[13] N. Bednar, N. Severino, and N. Adamovic, “Optical Simulation of Light Management in CIGS Thin-Film Solar Cells Using Finite Element Method,” *Appl. Sci.*, vol. 5, no. 4, pp. 1735–1744, 2015.

[14] N. Bednar, N. Severino, and N. Adamovic, “Front grid optimization of Cu (In, Ga) Se2 solar cells using hybrid modelling approach,” J. Renew. Sustain. Energy, vol. 7, no. 1, pp. 11201, 2015.

[15] A. Tamang, H. Sai, V. Jovanov, M. I. Hossain, K. Matsubara, and D. Knipp, “On the interplay of cell thickness and optimum period of silicon thin-film solar cells: Light trapping and plasmonic losses,” *Prog. Photovoltaics Res. Appl.*, vol. 24, no. 3, pp. 379–388, 2016.

[16] H. Tan, E. Moulin, F. T. Si, J. Schuttauf, M. Stuckelberger, O. Isabella, F. Haug, C. Ballif, M. Zeman, and A.H.M. Smets, “Highly transparent modulated surface textured front electrodes for high-efficiency multijunction thin-film silicon solar cells,” *Prog. Photovoltaics Res. Appl.*, vol. 23, no. 8, pp. 949–963, 2015.

[17] A. Hongsingthong, T. Krajangsang, A. Limmanee, K. Sriprapha, J. Sritharathikhun, and M. Konagai, “Development of textured ZnO-coated low-cost glass substrate with very high haze ratio for silicon-based thin film solar cells,” *Thin Solid Films*, vol. 537, pp. 291–295, 2013.

[18] K. Bittkau and A. Hoffmann, “Optical simulation of photonic random textures for thin-film solar cells,” in *Proceedings of SPIE*, vol. 9140, 2014.

[19] F. U. Hamelmann, “Transparent Conductive Oxides in Thin Film Photovoltaics,” in *Journal of Physics: Conference Series*, 2014, vol. 559, p. 1, 2016.

[20] V. K. Narasimhan and Y. Cui, “Nanostructures for photon management in solar cells,” Nanophotonics, vol. 2,no. 3, pp. 187–210 , 2013.

[21] M. C. Beard, J. M. Luther, and A. J. Nozik, “The promise and challenge of nanostructured solar cells,” *Nat. Nanotechnol.*, vol. 9, no. 12, pp. 951–954, 2014.

[22] A. Campa, J. Krc, and M. Topic, “Incoherent Propagation of Light in Coherent Models,” in the *proceedings of Comsol conference in Rotterdam*, no. 2, 2013.

[23] L. V. Mercaldo, I. Usatii, E. Bobeico, F. Russo, L. Lancellotti, and P. D. Veneri, “Optical Performance of Ag-based Back Reflectors with different Spacers in Thin Film Si Solar Cells,” *Energy Procedia*, vol. 84, pp. 221–227, Dec. 2015.

[24] N. Khoshsirat, N. A. Md Yunus, M. N. Hamidon, S. Shafie, and N. Amin, “Analysis of absorber layer properties effect on CIGS solar cell performance using SCAPS,” *Sci. Technol.*, vol. 23, no. 2, pp. 241–250, 2015.

[25] R. Khazaka, E. Moulin, M. Boccard, L. Garcia, S. Hanni, F. Haug, F. Meillaud, and C. Ballif , “Silver versus white sheet as a back reflector for microcrystalline silicon solar cells deposited on LPCVD-ZnO electrodes of various textures,” *Prog. Photovoltaics Res. Appl.*, vol. 23, no. 9, pp. 1182–1189, 2015.

[26] VT. J. Coutts, “High efficiency solar cells with CdS window layers,” Thin Solid Films, vol. 90, no. 4 p. 451–460 , 1982.

[27] A. Chemseddine and M. L. Fearheiley, “Improved CdS buffer/window layers for thin film solar cells,” *Thin Solid Films*, vol. 247, no. 1, pp. 3–7, Jul. 1994.

[28] M. Burresi, F. Pratesi, F. Riboli, and D. S. Wiersma, “Complex Photonic Structures for Light Harvesting,” *Adv. Opt. Mater.*, vol. 3, no. 6, pp. 722–743, 2015.

[29] B. von Roedern, “How do Buffer Layers Affect Solar Cell Performance and Solar Cell Stability,” in *MRS Proceedings*, vol. 668, no. 3, Cambridge Univ Press, 2001, pp. H6--9.

[30] C. Lathouwers, V. Singh, and S. Rajaputra, “Nano-structured Cadmium Sulfide Thin Films for Solar Cell Applications,” in *Southeastcon, 2013 Proceedings of IEEE*, pp. 1–8, 2013.

[31] M. Feifel, T. Rachow, J. Benick, J. Ohlmann, S. Janz, M. Hermle, F. Dimroth, and D. Lackner, “Gallium phosphide window layer for silicon solar cells,” *IEEE J. Photovoltaics*, vol. 6, no. 1, pp. 384–390, 2016.

[32] A. Micco, M. Pisco, A. Ricciardi, L.V. Mercaldo, L. Usatii, V.L. Ferrara, P.D. Veneri, A. Cutolo, and A. Cauano, “Plasmonic light trapping in thin-film solar cells: Impact of modeling on performance prediction,” *Materials (Basel).*, vol. 8, no. 6, pp. 3648–3670, 2015.

[33] X. Ye, S. Zou, K. Chen, J. Li, J. Huang, F. Cao, X. Wang, L. Zhang, X. Wang, M. Shen, and X. Su, “18.45%-Efficient Multi-Crystalline Silicon Solar Cells with Novel Nanoscale Pseudo-Pyramid Texture,” *Advanced Functional Materials*, vol. 24, no. 42, pp. 6708–6716, 2014.

[34] U. Palanchoke, V. Jovanov, H. Kurz, P. Obermeyer, H. Stiebig, and D. Knipp, “Plasmonic effects in amorphous silicon thin film solar cells with metal back contacts,” *Opt. Express*, vol. 20, no. 6, pp. 6340–6347, 2012.

[35] S. Ding, B. Eng, and P. Affairs, “Nanotechnology for single crystalline silicon solar cell applications,” Carleton University Ottawa, Ontario, 2015.

[36] A. Tamang, A. Hongsingthong, V. Jovanov, P. Sichanugrist, B. A. Khan, R. Dewan, M. Konagai, and D. Knipp, “Enhanced photon management in silicon thin film solar cells with different front and back interface texture,” *J. Renew. Sustain.*

Energy, vol. 7, no. 1, p. 11201, 2015.
[37] H. Sai, K. Saito, N. Hozuki, M. Kondo, “Relationship between the cell thickness and the optimum period of textured back reflectors in thin-film microcrystalline silicon solar cells,” *Appl. Phys. Lett.*, vol. 102, no. 5, p. 53509, 2013.
[38] A. Tamang, A.Hongsingthongb, P.Sichanugrist, V.Jovanov, H.T.Gebrewold, M.Konagai, D.Knipp, “On the potential of light trapping in multiscale textured thin film solar cells,” *Sol. Energy Mater. Sol. Cells*, vol. 144, no. January, pp. 300–308, 2016.
[39] J. Piprek, *Semiconductor optoelectronic devices: introduction to physics and simulation*. CALIFORNIA: Academic press, 2013.
[40] S. M. Sze, K. K. Ng, J.-P. Colinge, and C. A. Colinge, *Physics of Semiconductor Devices*. 2006.
[41] Ezenwa IA, “Synthesis and Optical Characterization of Zinc Oxide Thin Film,” *Res. J. Chem. Sci. Res.J.Chem.Sci*, vol. 2, no. 3, pp. 2231–606, 2012.
[42] F. U. Hamelmann, “Transparent Conductive Oxides in Thin Film Photovoltaics,” in *Journal of Physics: Conference Series*, 2014, vol. 559, p. 12016.
[43] J. Springer, A. Poruba, M. Vanecek, S. Fay, L. Feitknecht, N. Wyrsch, J. Meier, A. Shah, T. Repmann, O. Kluth, H. Stiebig, and B. Rech, “Improved optical model for thin film silicon solar cells,” in *Proceedings of the 17th European Photovoltaic Solar Energy Conference*, 2001, no. May 2017, pp. 1–6.
[44] M. Polyanskiy, "Refractive Index Database,” Available online: http://refractiveindex.info (accessed on 14 September 2015).
[45] X. Li, N. P. Hylton, V. Giannini, K.-H. Lee, N. J. Ekins-Daukes, and S. A. Maier, “Multi-dimensional modeling of solar cells with electromagnetic and carrier transport calculations,” *Prog. Photovoltaics Res. Appl.*, no. April, p. n/a-n/a, 2012.
[46] K. Emery, " AM1.5g solar spectrum irradiance data," Available online: http://rredc.nrel.gov/solar/spectra/am1.5 (accessed on 15 June 2015).
[47] R. Dewan, V. Jovanov, S. Hamraz, and D. Knipp, “Analyzing periodic and random textured silicon thin film solar cells by Rigorous Coupled Wave Analysis,” *Sci. Rep.*, vol. 4, no. August, p. 6029, 2014.
[48] V. Kumar, N. Singh, R. M. Mehra, A. Kapoor, L. P. Purohit, and H. C. Swart, “Role of film thickness on the properties of ZnO thin films grown by sol-gel method,” *Thin Solid Films*, vol. 539, pp. 161–165, 2013.
[49] J. Yoo and H. Soh, “Designing an optimal absorbing layer for thin-film solar cells,” *SPIE NewsRoom*, no. November 2012, pp. 6–8, 2016.
[50] A. Campa, J. Krc, and M. Topic, “Two approaches for incoherent propagation of light in rigorous numerical simulations,” *Prog. Electromagn. Res.*, vol. 137, no. February, pp. 187–202, 2013.
[51] S. Y. Lien, M.J. Yang, Y.S. Lin, C.F. Chen, P. H. Lin, C. H. Hsu, P. C. Huang, and Y. M. Shen, “Graded Buffer Layer Effect on Performance of the Amorphous Silicon Thin Film Solar Cells,” *Mater. Sci. Forum*, vol. 685, pp. 60–64, 2011.
[52] B. Von Roedern and G. H. Bauer, “Material Requirements for Buffer Layers Used to Obtain Solar Cells with High Open Circuit Voltages,” *MRS Proc.*, vol. 557, no. April, 1999.
[53] J. Fang, B. Liu, Y. Zhao, and X. Zhang, “Two-dimensional high efficiency thin-film silicon solar cells with a lateral light trapping architecture.,” *Sci. Rep.*, vol. 4, pp. 6169, 2014.
[54] M. N. Thomail, “Studying the Optical Properties of CdS Thin Films Prepared by Thermal Vacuum Evaporation Technique with a Different Thickness,” *J. Univ. anbar pure Sci.*, vol. 6, no. 1, pp. 1–4, 2012.